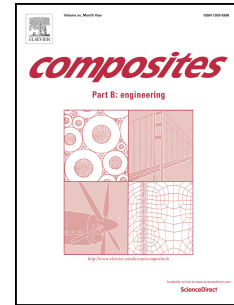


Accepted Manuscript

On the mechanical properties of monolithic and laminated nano-ceramic resin structures obtained by laser printing

B. Henriques, P. Pinto, F.S. Silva, M. Fredel, D. Fabris, J.C.M. Souza, O. Carvalho



PII: S1359-8368(17)30684-4

DOI: [10.1016/j.compositesb.2017.12.044](https://doi.org/10.1016/j.compositesb.2017.12.044)

Reference: JCOMB 5473

To appear in: *Composites Part B*

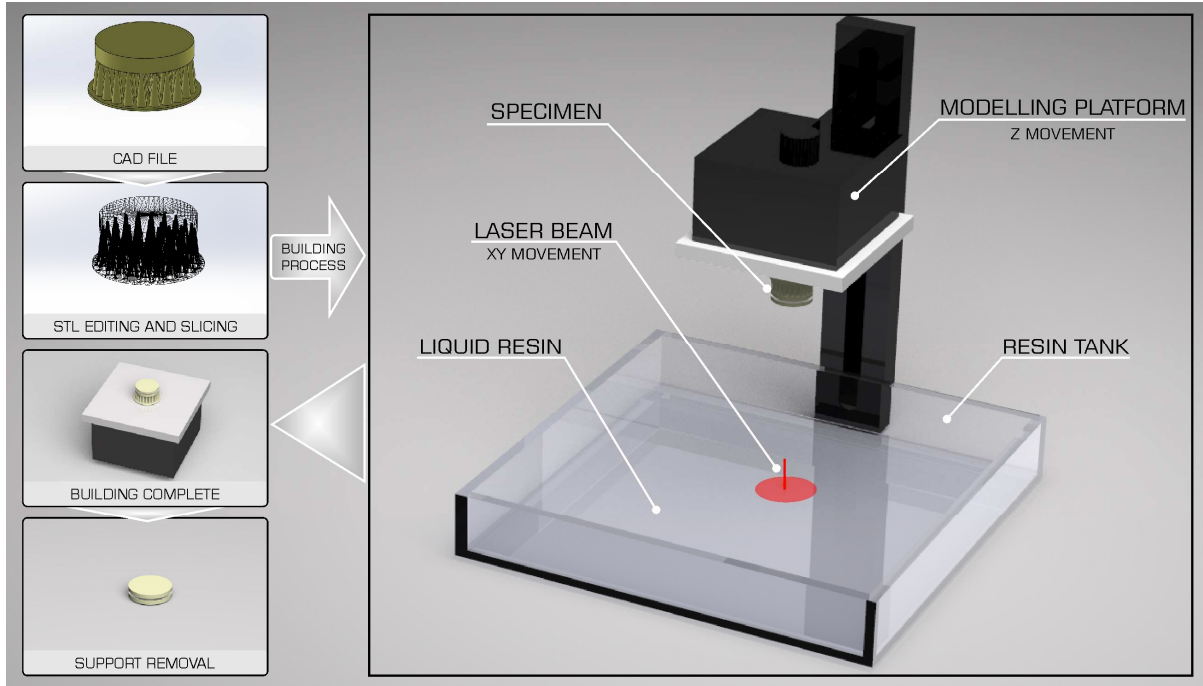
Received Date: 23 February 2017

Revised Date: 19 October 2017

Accepted Date: 18 December 2017

Please cite this article as: Henriques B, Pinto P, Silva FS, Fredel M, Fabris D, Souza JCM, Carvalho O, On the mechanical properties of monolithic and laminated nano-ceramic resin structures obtained by laser printing, *Composites Part B* (2018), doi: 10.1016/j.compositesb.2017.12.044.

This is a PDF file of an unedited manuscript that has been accepted for publication. As a service to our customers we are providing this early version of the manuscript. The manuscript will undergo copyediting, typesetting, and review of the resulting proof before it is published in its final form. Please note that during the production process errors may be discovered which could affect the content, and all legal disclaimers that apply to the journal pertain.



ACCEPTED MANUSCRIPT

On the mechanical properties of monolithic and laminated nano-ceramic resin structures obtained by laser printing

Henriques, B.^{1,2,3*}, Pinto, P¹., Silva F.S.¹, Fredel, M.², Fabris, D.² Souza, J.C.M.^{2,3}, Carvalho, O¹

¹Center for MicroElectroMechanical Systems (CMEMS-UMinho), University of Minho, Campus Azurém, Guimarães 4800-058, Portugal

²Ceramic and Composite Materials Research Group (CERMAT), Federal University of Santa Catarina (UFSC), Campus Trindade, Florianópolis/SC, Brazil

³School of Dentistry (DODT), Postgraduate Program in Dentistry (PPGO), Federal University of Santa Catarina, Campus Trindade, 88040-900, Florianópolis/SC, Brazil

***Corresponding author at:** Ceramic and Composite Materials Research Group (CERMAT), Federal University of Santa Catarina (UFSC), Campus Trindade, Florianópolis/SC, Brazil

E-mail address: brunohenriques@dem.uminho.pt (B. Henriques)

ABSTRACT

The purpose of this study was to evaluate the mechanical properties of laser printed monolithic and laminated nano ceramic resins (NCR) for dental prosthetic applications. Three different types of discs were produced by laser printing: monolithic NCR discs and laminated NCR discs with 100 μm (lamine_100) and 500 μm (lamine_500) resin interlayers (n=10). To assess the adhesion strength of the photosensitive resin used as interlayer to the NCR, cylindrical specimens were produced. The biaxial flexural strength and shear bond strength of the specimens was measured using a universal testing machine. Data statistically analysed by one-way ANOVA followed by Tukey HSD test ($\alpha=0.05$). The microstructure and fracture surfaces were analysed by SEM/EDS. Results were rationalized with finite element analysis (FEA). Lamine_100 specimens showed significantly higher flexural strength (~50%) than monolithic and Lamine_500 specimens ($p<0.05$). A good adhesion between the resin used as interlayer and the NCR was registered. FEA revealed a more favorable stress distribution in laminates with lower interlayer thickness. Modern CAD/CAM systems can be used in the direct manufacturing of correctly designed laminated structures displaying enhanced strength and damage tolerance relative to conventional monolithic ones, thereby positively impacting their clinical performance.

Keywords: nano-ceramic resin; laminated structures, flexural strength; laser printing; direct manufacturing;

1. Introduction

The developments seen over the past two decades in the Computer Aided Design coupled to Computer Aided Manufacturing (CAD/CAM) technologies applied to the fabrication of dental restorations has brought us to the era of digital dentistry [1,2]. The Cerec System (Sirona) was the first CAD/CAM system in dentistry, more than 25 years ago, with high success rates of the ceramic restorations produced. It is currently available in its fourth generation. Nowadays, it is possible to fabricate dental restorations from a wide range of materials to a high level of dimensional accuracy [3,4]. The most commonly used materials include zirconia, glass-ceramic and resin composites that are usually used in the form of blocks from where the restorations are milled [5,6]. The resin composite blocks for permanent restorations such as Lava Ultimate (3M ESPE) and Vita Enamic (Vita Zahnfabrik) have been recently developed as materials for CAD/CAM production and have the advantages over ceramic materials of requiring lower processing times and being easily adjusted, milled and repaired [7–10]. The advantages over traditional resin composites polymerized in situ are their greater filler volume fractions that impart better mechanical properties as well as their enhanced dimensional accuracy due to the absence of an in-situ occurrence of curing shrinkage [11,12]. Despite both being resin composite materials, Lava Ultimate and Vita Enamic have different microstructures. The first consist of discrete dispersed and inorganic filler particles (silica and zirconia) embedded in a polymer matrix, and the latter is a polymer-infiltrated-ceramic-network material (PICN), which consists in a feldspathic porcelain interpenetrating phase (86 wt.%) infiltrated by a acrylate-polymer (14 wt.%) [13,14]. Wear tests have shown that the volume loss on antagonist enamel produced by resin composites were lower than that produced by zirconia and glass-ceramics [8,15–17].

Despite the term CAD/CAM in the dental restorative field is often associated to the milling technology it is much broader and includes subtractive and additive manufacturing technologies. The composite resin Temporis (DWS, Italy) is a photosensitive nano-resin ceramic commercialized by DWS for direct manufacturing of long-term temporary crowns and bridges. The restorations are fabricated in the DigitalWax® machines from a 3D CAD file controlled by a specific software that controls a laser source of ultraviolet radiation that solidify in a layerwise fashion the photosensitive resin. The DigitalWax®

stereolithography machines are characterized by a transparent resin tank which allows the laser beam to pass through it, and a laser scanning unit placed directly under the tank.

The adhesively laminated ceramics have been shown to improve the mechanical properties of brittle ceramics in applications such as thermal barrier coatings [18,19], automotive windscreens [20–22] and lately in dental feldspathic ceramics [23]. It has been demonstrated elsewhere that the lamination of glass substrates produces a reduction of the structure stiffness whilst maintaining or increasing the flexural strength [21,24–26]. The toughening mechanism of ceramic laminated by a polymer adhesive interface has been described as the capacity of the laminating adhesive (interlayer) to absorb energy elastically and to allow shear transfer, i.e. deflection of the stresses away from the point of application. When a crack is formed and propagates through the adhesive interlayer, the strain of the adhesive helps to arrest the crack propagation. The literature involving laminated dental ceramics is scarce. Costa et al. (2008) [23] hypothesized whether the adhesive lamination of ceramic materials could offer mechanical advantages over monolithic structures and improve clinical outcomes. They found that ceramic lamination increased the damage tolerance of the structures and that cracks growth near the interlayer could be limited or arrested.

Besides producing and testing monolithic nano ceramic resin by laser printing, the versatility of the DigitalWax® stereolithography system, which allows a quick change of material and therefore the fabrication of multimaterial parts, has lead us to the possibility of producing and testing laminate nano ceramic resins with a photosensitive resin used as elastic interlayer between the monolithic nano ceramic resin structures. The influence of an elastic interlayer on the mechanical properties of the laminated material, as well as the adhesion of the resin to the nano ceramic resin, has been assessed. The results were rationalized with Finite Element Analysis.

2. MATERIALS AND METHODS

2.1. Materials

The materials used in this study were a nano ceramic resin (Irix, DWS, Italy) and a photosensitive resin (DC600, DWS, Italy). The mechanical and physical properties of the materials used in this study as well as other resin composites for CAD/CAM manufacturing are presented in Table 1.

Table 1 – Mechanical properties of resin based materials					
	Flexural Strength [MPa]	Young's modulus (GPa)	Fracture toughness [MPa·m ^{1/2}]	Hardness [HV/GPa]	Density [g/cm ³]
TEMPORIS (DWS, Italy)	93	2.7	---	---	---
LavaTM Ultimate 3M*	204±19	12.77±0.9 9	2.02±0.15	102 [8]	---
Vita Enamic*	150-160	30	1.5	157 [8]	2.1
Dentin	---	16-20 [27,28]	2.2-3.1 [29,30]	0.6-0.92 [29,31]	1.96-2.4 [32]
Enamel	----	48-105.5 [33,34]	0.6-1.5 [34,35]	3-5.3 [28,36]	3.02 [36]
* According to manufacturer					

2.2. Manufacturing of the discs and cylinders for testing

Three types of disc geometries were fabricated for this study (Figure 1): monolithic nano ceramic resin (NCR) discs with 14 mm of diameter and 2.5 mm of height (n=10); NCR discs with 14 mm of diameter,

2.5 mm of height and with a resin interlayer of 500 μm of thickness, hereafter referred as laminate_500; and NCR discs with 14 mm of diameter, 2.1 mm of height and with a resin interlayer of 100 μm of thickness, hereafter referred as laminate_100. The discs were fabricated from a 3D CAD file in a laser printer machine (DWS, Italy) according to the schematic presented in Figure 2. All models underwent an additional exposure to a specific UV light source in a UV curing unit (S2 model, Digital Wax, Italy) for consolidation and stabilization of their structure.

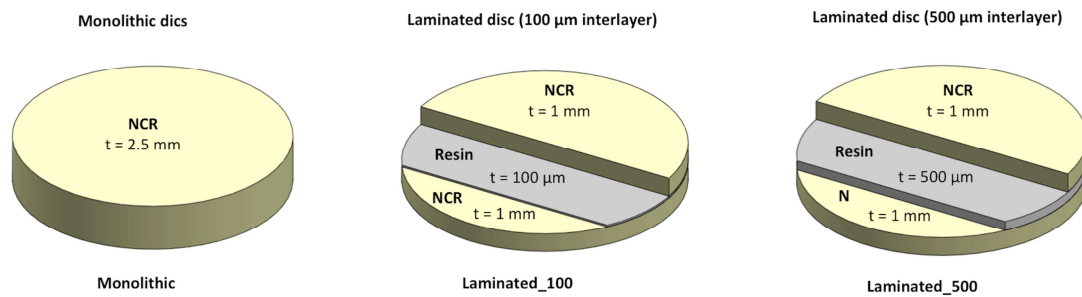


Figure 1 - Building design of nano ceramic resin (NCR) monolithic and laminated discs manufactured by laser printing.

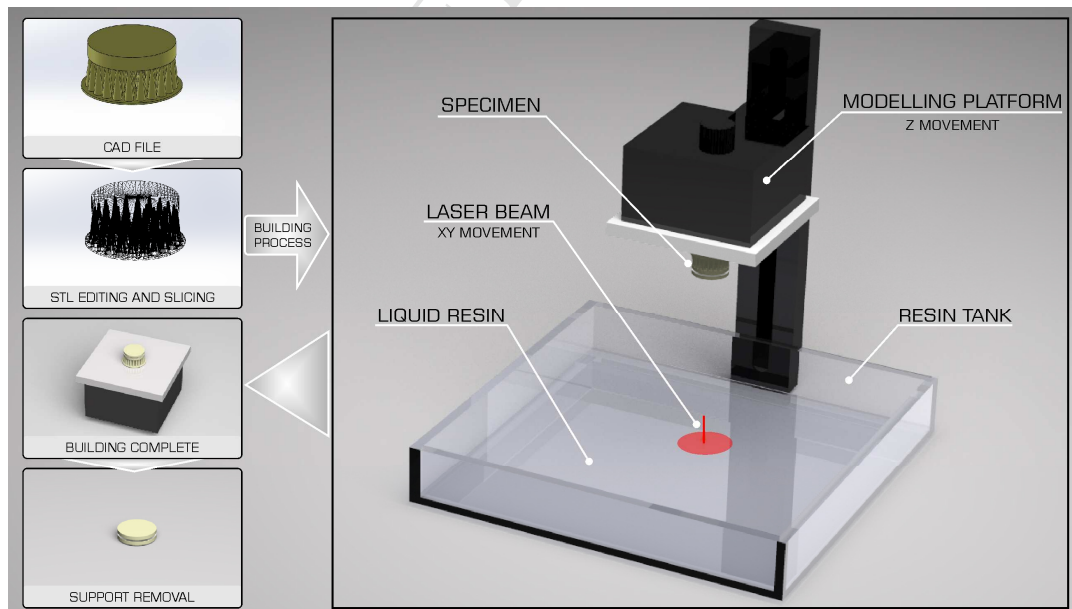


Figure 2 – Schematic of the stereolithography process used to fabricate the nano ceramic resin discs. The

model with the desired geometry is first created in CAD software. The STL file is then uploaded to the CAM software linked to the stereolithography machine and the building process starts.

In order to assess the shear strength of the base materials this study, ten cylinders of each material with 8 mm diameter and 8 mm height were printed. For reaching the success of a laminated material it is important to have a good adhesion between the layered materials. Therefore, in order to assess bond strength between the two materials [37–39], ten cylinders with 8 mm diameter and 4 mm of each material, making a total height of 8 mm were printed. The nano ceramic resin part was the first to be printed and the photosensitive resin was afterwards printed on its topside once the 4 mm height had been reached.

2.3. Determination of Biaxial Flexural Strength

The biaxial flexural strength tests of monolayered and trilayered discs were determined in a piston on three balls test setup at room temperature ($21 \pm 1^\circ\text{C}$) using an universal testing machine (Instron 8874, MA, USA) with a load cell of 25kN, and at a loading rate of 1mm/min. The discs were positioned in the sample holder on top of the three supporting balls and the upper surface of the discs were centrally loaded with a 1.6 mm diameter pin mounted in the crosshead of the testing machine. The load at fracture and the number of fracture fragments were recorded for each specimen.

The biaxial strength was calculated using the Hsueh et al.'s formulae, which is derived from ISO 6872 standard formulae, and showed good accuracy in determining the stress distribution in our multilayered discs [40]. The stress moment in a multilayer disc is described by:

$$\sigma_i = \frac{E_i(z-z^*)M}{(1-\nu_i)(1+\nu_{ave})D^*} \quad (3)$$

where E_i and ν_i are the Young's modulus and the Poisson ratio of the i th layer, M is the biaxial bending moment per unit length, z^* is the position of the neutral plane, D^* is the flexural rigidity and ν_{ave} is the average Poisson's ratio. E_i and ν_i are calculated by Eq. (2), and the others variables are given by:

$$z^* = \frac{\sum_{i=1}^n \frac{E_i t_i}{1-\nu_i} (h_{i-1} + \frac{t_i}{2})}{\sum_{i=1}^n \frac{E_i t_i}{1-\nu_i^2}} \quad (4)$$

$$D^* = \sum_{i=1}^n \frac{E_i t_i}{1-\nu_i^2} \left[h_{i-1}^2 + h_{i-1} t + \frac{t_i^2}{3} - \left(h_{i-1} + \frac{t_i}{2} \right) z^* \right] \quad (5)$$

$$\nu_{ave} = \frac{1}{h_n} \sum_{i=1}^n \nu_i t_i \quad (6)$$

$$M = \frac{-P}{8\pi} \left\{ (1 + \nu_{ave}) \left(1 + 2 \ln \frac{a}{c} \right) + (1 - \nu_{ave}) \left[\left(1 - \frac{c^2}{2a^2} \right) \frac{a^2}{R^2} \right] \right\} \quad (7)$$

The disc with radius R is supported on three balls that are evenly spread on a circle with a radius a and loaded by a piston at the center with a radius c .

For $n=1$ (one layer only), Hsueh et al. formula is reduced to the ISO 6872 monolayered disc formula. Therefore, the formula can be used to calculate the stress moment for both monolayered and multilayered discs.

2.4. Analysis of the microstructure and fracture surfaces

The microstructure of the nano ceramic resin was analyzed by field emission guns electron microscopy (FEG-SEM; NOVA 200 Nano SEM, FEI Company). For that, samples were embedded in self-curing resin, wet-ground using grit SiC sand-papers down to 4000 Mesh and polished with diamond paste (1 μ m). Afterwards they were gold coated. The fracture surfaces were gold sputtered and examined by SEM (TM3030, Hitachi, Japan) at operating voltages ranging between 5 and 10kV.

2.5. Statistical analysis

The results were analyzed using one-way ANOVA followed by Tukey HSD multiple comparison test. The Shapiro-Wilk test was first applied to test the assumption of normality. P values lower than 0.05 were considered statistically significant.

2.6. Finite element method

Finite element method (FEM) was used to simulate the stress distribution in the biaxial flexural test. A two dimensional axisymmetric model was used to simplify the calculations. The simulations were carried out with the commercial software Comsol Multiphysics. A constant force was applied at the superior edge of the piston, which then transfers the force to the disc. The supporting ring was fully constrained, and the piston movement was restricted to move only in the vertical axis. All layers were considered to remain bonded during the simulation. A fine mesh with free triangular elements, with maximum size of 0.05 mm, was used. The elements were refined near the region where the stress was the highest, i.e. in the region near the z-axis, in a way that each layer had 20 elements at its edge, except layers smaller than 0.1 mm, which had 10 elements. A mesh refinement study was performed to ensure the accuracy of the simulated results. Using extremely fine mesh was necessary to avoid singularities in the model. In this study, the friction between the disc, the supports and the piston was ignored.

3. RESULTS

Figure 3 shows the microstructure of the nano ceramic resin at high magnification where white phases, corresponding to inorganic particles, can be detected within a polymeric matrix appearing as the dark phase. The EDS presented in Figure 3 identified the inorganic phase as being SiO_2 and Al_2O_3 particles.

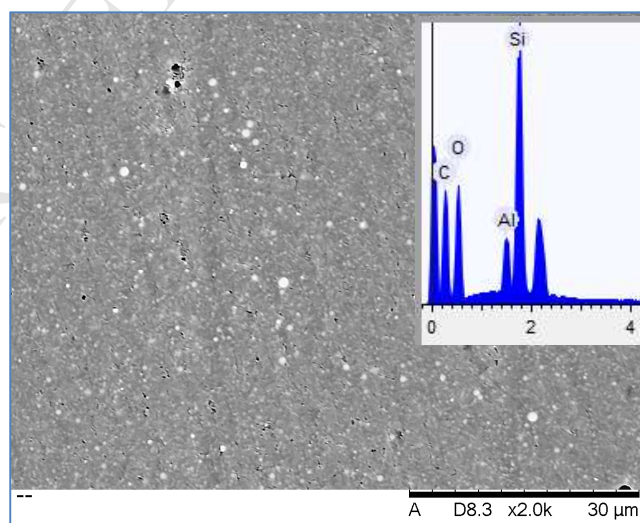


Figure 3 – Micrograph and EDS analysis of the resin nano ceramic material showing dispersed SiO_2 and Al_2O_3 nanoparticles embedded in a polymeric matrix. Residual porosity can be detected.

Figure 4A shows a plot of the biaxial flexural strength of the monolithic nano ceramic resin and laminate materials with 100 μm and 500 μm resin interlayers. The statistical analysis revealed significant differences between the flexural strength of the different discs ($p < 0.05$). The laminated_100 discs (128.9 ± 13.6 MPa) showed significantly higher flexural strength than the monolithic (86.1 ± 13.9 MPa) and the laminated_500 discs (78.3 ± 3.8 MPa) ($p < 0.05$). The flexural strength of the laminated_500 discs decreased significantly relative to the monolithic discs ($p < 0.05$). Figure 4B shows the deflection at fracture exhibited by the different specimens. The statistical analysis revealed no significant difference between the groups ($p > 0.05$). The stiffness results are shown in Figure 4C. The statistical analysis did not reveal significant differences between the groups ($p > 0.05$)

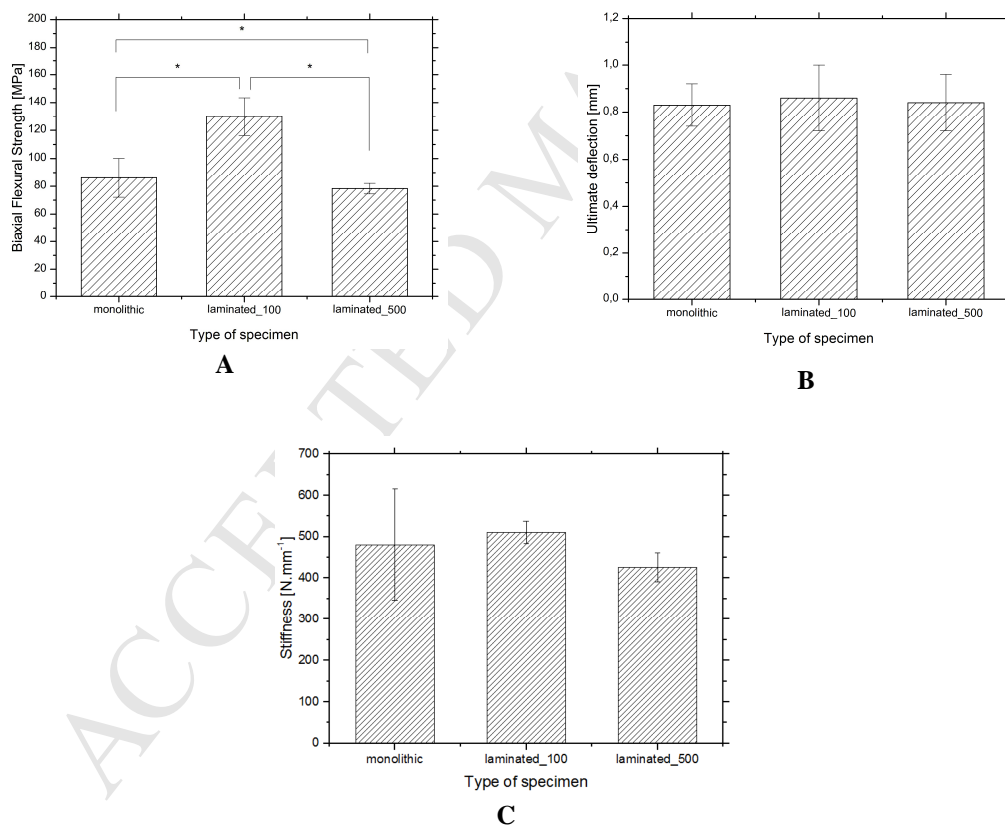


Figure 4 – Fracture strength (A), ultimate deflection (B) and stiffness (C) of the different specimens: monolithic nano ceramic resin; laminated nano ceramic resin with 100 μm resin interlayer; laminated nano ceramic resin with 500 μm resin interlayer. The asterisk (*) indicates significant differences between

the groups.

The shear strength of the nano ceramic resin and of the photosensitive resin used as interlayer in laminate materials, as well as the shear bond strength between both materials are presented in Figure 5. The shear strength of the photosensitive resin was significantly lower than that of the nano ceramic resin (by ~4 times). The shear bond strength between both materials was in the range of the photosensitive resin cohesive strength values, revealing an excellent adhesion between the two materials.

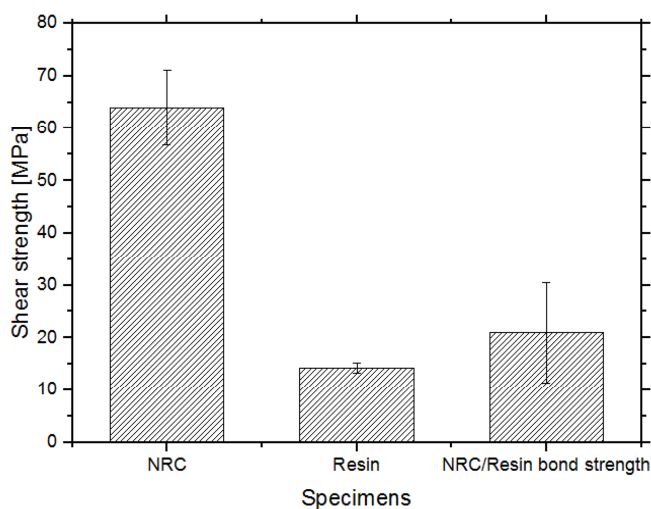


Figure 5 – Plot of the shear strength of nano ceramic resin and the photosensitive resin, and the shear bond strength of the two materials.

The fracture surface of a nano ceramic resin specimen veneered by photosensitive resin after the shear bond strength test is presented in Figure 6. It can be seen in that remnants of the photosensitive resin remained at the fracture surface after testing, confirming the good adhesion exhibited by the two materials at the shear bond strength test.

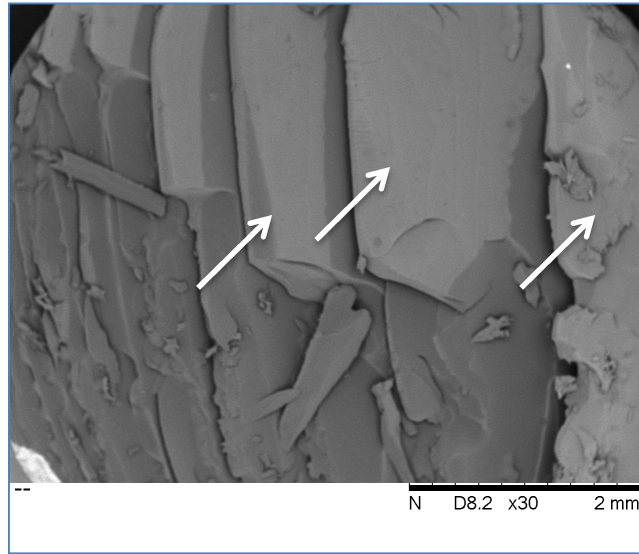


Figure 6 – Fracture surface of the nano ceramic resin veneered by photosensitive resin after shear bond strength test showing remnants of the photosensitive resin at the fracture surface.

Figure 7 shows the fracture surface of the specimens of the different groups and it can be seen that, in all specimens, failure started from the bottom part of the discs, which corresponds to the tensile surface in the flexural test. The fracture surfaces revealed typical fracture patterns of ceramic materials, namely the presence of hackle lines (HL) and compression curl (CC). The compression curl is a feature often seen in specimens subjected to flexural tests, as the stress gradient formed makes the crack to slow down and to change direction, thus creating a curve. The fracture origin is at the opposite direction to the compression curl [41].

The microstructural hackles are pronounced lines that form without a specific cause, usually due to variations in material's microstructure. Ceramics tend to develop such lines when either a mirror region or other characteristic marks are absent, and it occurs when the strength is low or in the presence of high porosity. It might arise as the only mark on the fracture surface indicating the orientation of the crack propagation [41].

The fracture micrographs of the laminated specimens did not show delamination signs occurring at the different layers after the bending tests, thus evidencing a good adhesion between the interlayer and the outer NRC layers. The fracture surfaces also revealed the absence of detectable porosity within the discs.

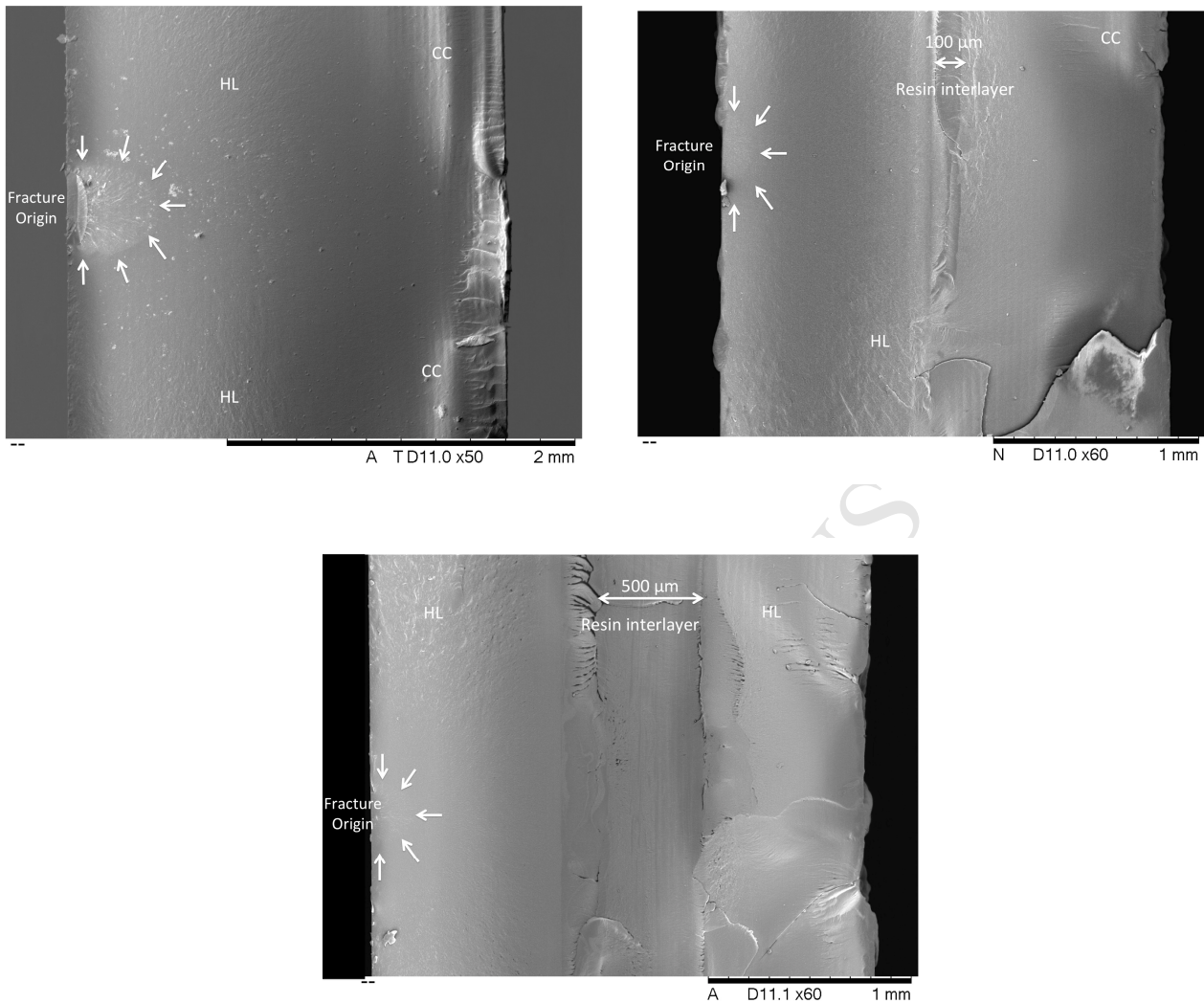


Figure 7 – SEM micrographs of fracture surfaces of specimens from the different groups: A) monolithic nano ceramic resin; B) laminated nano ceramic resin with 100 μm resin interlayer; C) laminated nano ceramic resin with 500 μm resin interlayer. The presence of typical brittle marks such as compression curl (CC) and hackle lines (HL) can be observed. The arrows indicate the critical defect.

Figure 8A shows a comparison of the stress distribution within the different discs subjected to a biaxial flexural test when a fixed load of 200N is applied in the center of the disc. Figure 8B plots the stress distribution along the thickness in the center of the discs, where the maximum stresses were registered. It can be seen that the maximum tensile stresses occur at the bottom part of the discs for monolithic and laminated_100 discs. The laminated_500 discs exhibit the maximum tensile stresses at

the interface between the upper NRC disc and the resin interlayer. Additionally, laminated_100 and laminated_500 present a considerable stress mismatch at the interface between the NRC upper disc and the resin interlayer. The analysis of the maximum tensile stresses at the bottom side of the disc show that monolithic discs present the lowest values and the laminated_100 discs the highest.

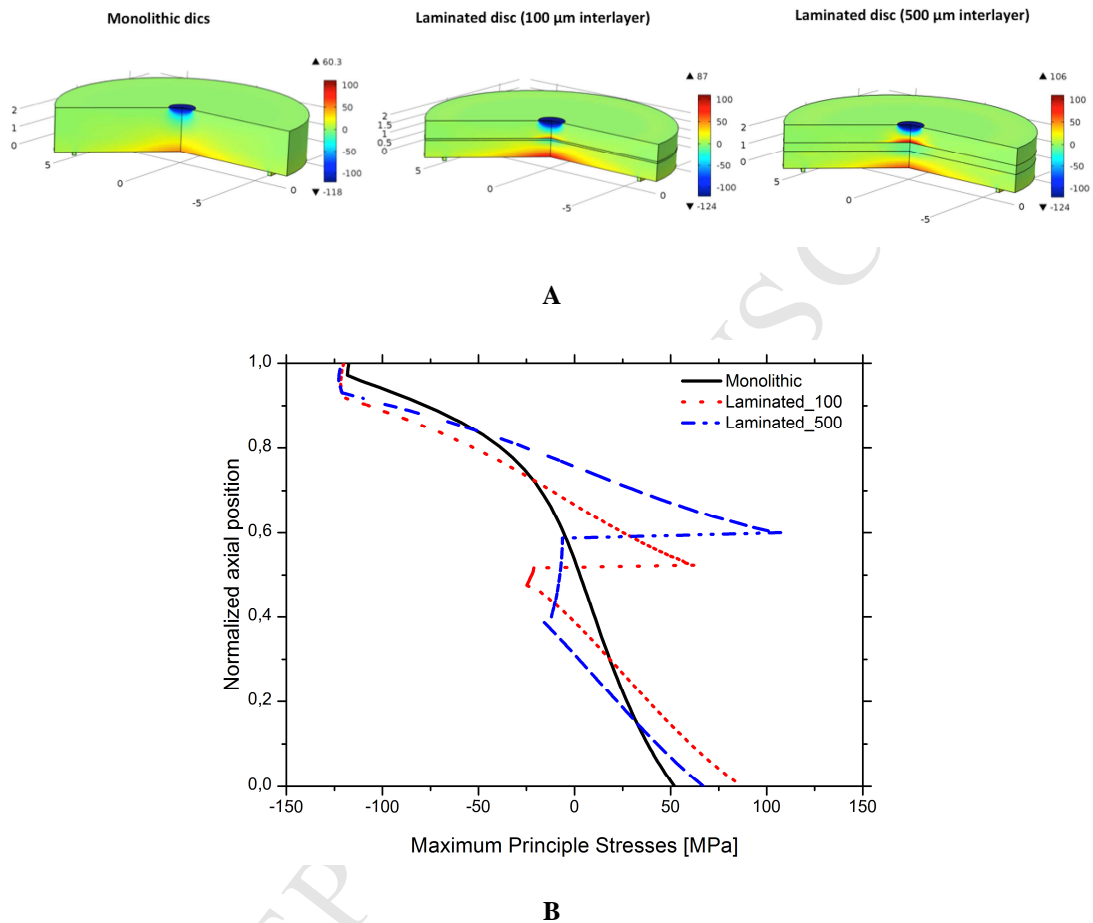


Figure 8 – Maximum principle stresses in monolithic and laminated discs under a biaxial flexural test with a centrally applied load of 200 N. A) Stress distribution map; B) Stress profile measure at the center of the discs.

4. DISCUSSION

This study has been conducted with the main purpose of assessing the feasibility of direct printing monolithic and laminated nano ceramic resins for temporary dental restorations as well as their mechanical behavior.

The flexural strength of the monolithic discs was found to be similar to that reported by the manufacturer (Table 1) and is in the range of values reported in literature for composite resins [42]. These values are, however, lower than the strength values reported for composite resins used in the form of blocks for dental CAD/CAM systems such as the Lava Ultimate and also lower than Vita Enamic, which belongs to the class of interpenetrating phase composites (IPCs) [43–45] (Table 1). Unlike the conventional composite resins, as is the case of the nano resin composite used in this study, which consists of discrete dispersed and isolated inorganic filler particles with different sizes, shapes and filling degree embedded in a polymeric matrix [46], the IPCs consists of two continuous interpenetrating networks [44], one ceramic (feldspar) and the other a polymer (methacrylates) in the case of Enamic composite [5,6,13]. The additional resistance of the IPCs is attributed to the reinforcing phase that distributes stresses effectively in all directions and also to the distribution of such enhanced resistance by several breakdown phenomena [43]. Hence, the polymer phase provides resistance to crack propagation by bridging cracks introduced to the brittle material.

The laminate specimens showed divergent behaviors, with the laminate_100 presenting significantly higher flexural strength relative to monolithic specimens and the laminate_500 decreasing significantly the same flexural strength relative to monolithic specimens, although in the latter case the resistance values were close. These results can be rationalized with the finite element analysis presented in Figure 8 where the stress distribution across the discs' thickness for a fixed load of 200N is plotted. The FE analysis revealed a continuous and monotonic stress distribution across the thickness of the monolithic discs with the higher tensile stresses occurring at the bottom surface, as already expected. On the other hand, stresses distribution in laminated discs showed a very different profile. High tensile stresses were also developed at the interlayer region, with a high stress mismatch being created at the interface between the top nano ceramic resin disc and the resin interlayer. It must be highlighted that, conversely to what was seen for laminate_100 specimens, the maximum tensile stresses in laminate_500 specimens were present at the interlayer region rather than at the bottom side of the disc, which indicates this site as a critic point where cracks may form and propagate.

Concerning stresses in laminate_100 discs, despite a stress mismatch is also created at the interlayer's region, the highest tensile stress values were also seen at the bottom surface, similarly to the monolithic discs. The significantly higher flexural strength displayed by the laminate_100 shows that this design

configuration allowed to achieve the desired toughening mechanics typical of ceramic laminated by a polymer adhesive interface based on the ability of the laminating adhesive (interlayer) to absorb energy elastically and to allow shear transfer. This phenomenon is well seen in the fracture surfaces of laminate specimens (Figure 7) where the crack formed at the tensile stresses propagates freely until it reaches the adhesive interlayer. Here the strain of the adhesive helps to arrest the crack propagation, decreasing the propagation speed and dissipating energy. The deviation in the crack direction caused by the resin interlayer and visible in the fracture micrographs reinforces the evidences of toughening effect seen in laminated discs (Figure 7). Costa et al. [23] demonstrated that cracks formed after indentations made in the ceramic, adjacent to the resin interlayer, tend to propagate parallel to the interlayer and no longer in a radial direction towards the surface, thus exhibiting a toughening mechanism resulting from the crack arrest in the resin interlayer.

The interlayer's thickness, in the range of values used in this study, played a significant role in the flexural strengths of the laminate discs. The interlayer's elastic modulus and thickness have been shown to influence the laminate glass materials (LG) [25]. For example, Hidallana-Gamage et al. (2015) demonstrated that there is a critic value for the interlayer's thickness and elastic modulus, above of which there is an improved stress distribution on both glass and interlayer, and minimization of the damage of the interlayer. Therefore, laminates with higher interlayer thickness and stiffness tend to exhibit higher load carrying capacity than those with smaller E and thickness. In our study, however, different tendency was found for the type of materials used. The laminates with thicker interlayer (laminata_500) exhibited significantly lower flexural strength than those with thinner interlayers (laminata_100). The explanation for the divergent results might be related to the different materials employed in both studies and by the different interlayers thickness range, which was 100 μm – 500 μm in our study and 760 μm -2280 μm in Hidallana-Gamage et al. study [25].

The resin used as interlayer in the laminate discs had a very low elastic modulus (~172 MPa), which can explain the high tensile stresses originated at the interlayer region of the laminate discs. Hence, the application of a stiffer interlayer is believed to result in enhanced strength of the laminate discs. Similar findings have been reported for ceramic restorations where the stiffness of the substrate including the luting cement have been shown to play an important role in the fracture resistance [47–49]. It has been demonstrated that the failure triggered by the development of tensile stresses is highly sensitive to the

ratios of elastic moduli between the restorative material, luting agent and substrate [47,50,51]. It has been therefore suggested that the improvement of clinical performance would be achieved by increasing the resin cement modulus and assuring a good bonding [49].

One important factor in laminate ceramics is achieving a good adhesion between the ceramic discs and the resin interlayer. It has been reported that well-luted specimens display usually higher fracture resistance [52–55]. This would lead to bridging effects on the interfacial surface defects, thus restricting and resisting against the propagation of cracks from the internal surface of the bonded resin [47,53,56] and leading to a higher fracture resistance.

The ultimate deflection (maximum deflection at failure) did not differ significantly within the different groups. This behavior is in accordance with Hidallana-Gamage et al. [25] findings, which have shown that maximum deflection did not vary with the interlayers thickness when slow deformation rates were used. Additionally, the stiffness of laminates did not show to significantly differ from the monolithic specimens, which contrast to typical behavior of laminated ceramics [23–25]. Differences in the base materials and in the processing technique used in this study might be in the origin of such behavior.

Finally, considering the results reported above, it can be seen that the laminated nano ceramic resin with 100 μm resin interlayer displayed significantly enhanced strength relative to the monolithic material (~50%), without compromising the ultimate deflection and the original stiffness.

5. Conclusions

This study assessed the feasibility of production and the mechanical properties of laminate nano ceramic resin obtained by CAD/CAM laser process. Within the limitations of the present study, the following conclusions can be drawn:

1. Laminate nano ceramic resin (NCR) specimens were successfully produced using a CAD/CAM laser assisted process;
2. A good adhesion between the resin and the NCR discs was registered, evidenced by the high shear bond strength results;
3. The laminate specimens with 100 μm thickness interlayers displayed significantly higher flexural strength (~50%) than those exhibited by the monolithic specimens ($p < 0.05$).

4. Direct manufactured laminated materials arise as a promising alternative to conventional monolithic ones in the production of dental structures with enhanced strength and damage tolerance.

ACKNOWLEDGEMENTS

This study was supported by FCT-Portugal (UID/EEA/04436/2013, NORTE-01-0145-FEDER-000018 - HAMaBICo) and CNPq-Brazil (PVE/CAPES/CNPq/407035/2013-3)



REFERENCES

- [1] F. Beuer, J. Schweiger, D. Edelhoff, Digital dentistry: an overview of recent developments for CAD/CAM generated restorations., *Br. Dent. J.* 204 (2008) 505–511.
doi:10.1038/sj.bdj.2008.350.
- [2] R.L.P. Santos, F.S. Silva, R.M. Nascimento, J.C.M. Souza, F. V. Motta, O. Carvalho, et al., Shear bond strength of veneering porcelain to zirconia: Effect of surface treatment by CNC-milling and composite layer deposition on zirconia, *J. Mech. Behav. Biomed. Mater.* 60 (2016) 547–556.
doi:10.1016/j.jmbbm.2016.03.015.
- [3] G. Bosch, A. Ender, A. Mehl, A 3-dimensional accuracy analysis of chairside CAD/CAM milling processes, *J. Prosthet. Dent.* 112 (2014) 1425–1431. doi:10.1016/j.prosdent.2014.05.012.
- [4] T.A. Hamza, R.M. Sherif, In vitro evaluation of marginal discrepancy of monolithic zirconia restorations fabricated with different CAD-CAM systems, *J. Prosthet. Dent.* (2016).
doi:10.1016/j.prosdent.2016.09.011.
- [5] R. Belli, M. Wendler, D. de Ligny, M.R. Cicconi, A. Petschelt, H. Peterlik, et al., Chairside CAD/CAM materials. Part 1: Measurement of elastic constants and microstructural characterization, *Dent. Mater.* (2016). doi:10.1016/j.dental.2016.10.009.
- [6] M. Wendler, R. Belli, A. Petschelt, D. Mevec, W. Harrer, T. Lube, et al., Chairside CAD/CAM materials. Part 2: Flexural strength testing, *Dent. Mater.* (2016).

- doi:10.1016/j.dental.2016.10.008.
- [7] J. Min, D.D. Arola, D. Yu, P. Yu, Q. Zhang, H. Yu, et al., Comparison of human enamel and polymer-infiltrated-ceramic-network material " ENAMIC " through micro-and nano-mechanical testing, *Ceram. Int.* 42 (2016) 10631–10637. doi:10.1016/j.ceramint.2016.03.160.
- [8] N.C. Lawson, R. Bansal, J.O. Burgess, *Wear*, strength, modulus and hardness of CAD/CAM restorative materials, *Dent. Mater.* 32 (2016) e275–e283. doi:10.1016/j.dental.2016.08.222.
- [9] L. Zhi, T. Bortolotto, I. Krejci, Comparative in vitro wear resistance of CAD/CAM composite resin and ceramic materials, *J. Prosthet. Dent.* 115 (2016) 199–202.
doi:10.1016/j.prosdent.2015.07.011.
- [10] A.C. Diniz, R.M. Nascimento, J.C.M. Souza, B.B. Henriques, A.F.P. Carreiro, Fracture and shear bond strength analyses of different dental veneering ceramics to zirconia., *Mater. Sci. Eng. C. Mater. Biol. Appl.* 38 (2014) 79–84. doi:10.1016/j.msec.2014.01.032.
- [11] S. Nandini, Indirect resin composites., *J. Conserv. Dent.* 13 (2010) 184–194. doi:10.4103/0972-0707.73377.
- [12] H.Y. Marghalani, Effect of filler particles on surface roughness of experimental composite series., *J. Appl. Oral Sci.* 18 (2010) 59–67. doi:10.1590/S1678-77572010000100011.
- [13] A. Della Bona, P.H. Corazza, Y. Zhang, Characterization of a polymer-infiltrated ceramic-network material, *Dent. Mater.* 30 (2014) 564–569. doi:10.1016/j.dental.2014.02.019.
- [14] A. Coldea, M. V. Swain, N. Thiel, Mechanical properties of polymer-infiltrated-ceramic-network materials, *Dent. Mater.* 29 (2013) 419–426. doi:10.1016/j.dental.2013.01.002.
- [15] J.C.M. Souza, A.C. Bentes, K. Reis, S. Gavinha, M. Buciumeanu, B. Henriques, et al., Abrasive and sliding wear of resin composites for dental restorations, *Tribol. Int.* 102 (2016) 154–160.
doi:10.1016/j.triboint.2016.05.035.
- [16] R. Belli, E. Geinzer, A. Muschweck, A. Petschelt, U. Lohbauer, Mechanical fatigue degradation of ceramics versus resin composites for dental restorations, *Dent. Mater.* 30 (2014) 424–432.
doi:10.1016/j.dental.2014.01.003.
- [17] H. Chadda, B.K. Satapathy, A. Patnaik, A.R. Ray, Mechanistic interpretations of fracture toughness and correlations to wear behavior of hydroxyapatite and silica/hydroxyapatite filled bis-GMA/TEGDMA micro/hybrid dental restorative composites, *Compos. Part B Eng.* 130

- (2017) 132–146. doi:10.1016/j.compositesb.2017.07.069.
- [18] M. Tamura, M. Takahashi, J. Ishii, K. Suzuki, M. Sato, K. Shimomura, Multilayered Thermal Barrier Coating for Land-Based Gas Turbines, *J. Therm. Spray Technol.* 8 (1999) 68–72. doi:10.1361/105996399770350584.
- [19] X.Q. Cao, R. Vassen, D. Stoeber, Ceramic materials for thermal barrier coatings, *J. Eur. Ceram. Soc.* 24 (2004) 1–10. doi:10.1016/S0955-2219(03)00129-8.
- [20] H.S. Norville, K.W. King, J.L. Swofford, Behavior and Strength of Laminated Glass, *J. Eng. Mech.* 124 (1998) 46–53. doi:10.1061/(ASCE)0733-9399(1999)125:8(985).
- [21] G.I. Shim, S.H. Kim, D.L. Ahn, J.K. Park, D.H. Jin, D.T. Chung, et al., Experimental and numerical evaluation of transparent bulletproof material for enhanced impact-energy absorption using strengthened-glass/polymer composite, *Compos. Part B Eng.* 97 (2016) 150–161. doi:10.1016/j.compositesb.2016.04.078.
- [22] S. Chen, M. Zang, D. Wang, S. Yoshimura, T. Yamada, Numerical analysis of impact failure of automotive laminated glass: A review, *Compos. Part B Eng.* 122 (2017) 47–60. doi:10.1016/j.compositesb.2017.04.007.
- [23] A.K.F. Costa, R.D. Kelly, G.J.P. Fleming, A.L.S. Borges, O. Addison, Laminated ceramics with elastic interfaces: A mechanical advantage?, *J. Dent.* 43 (2015) 335–341. doi:10.1016/j.jdent.2014.12.012.
- [24] T. Serafinavicius, A.K. Kvedaras, G. Sauciunenas, Bending behavior of structural glass laminated with different interlayers, *Mech. Compos. Mater.* 49 (2013) 437–446. doi:10.1007/s11029-013-9360-4.
- [25] H.D. Hidallana-Gamage, D.P. Thambiratnam, N.J. Perera, Influence of interlayer properties on the blast performance of laminated glass panels, *Constr. Build. Mater.* 98 (2015) 502–518. doi:10.1016/j.conbuildmat.2015.08.129.
- [26] G. Castori, E. Speranzini, Structural analysis of failure behavior of laminated glass, *Compos. Part B Eng.* 125 (2017) 89–99. doi:10.1016/j.compositesb.2017.05.062.
- [27] B.R. Hairul Nizam, C.T. Lim, H.K. Chng, A.U.J. Yap, Nanoindentation study of human premolars subjected to bleaching agent, *J. Biomech.* 38 (2005) 2204–2211. doi:10.1016/j.jbiomech.2004.09.023.

- [28] B.R. Lawn, Y. Deng, V.P. Thompson, Use of contact testing in the characterization and design of all-ceramic crownlike layer structures: A review, *J. Prosthet. Dent.* 86 (2001) 495–510.
doi:10.1067/mpr.2001.119581.
- [29] B.R. Lawn, J.J.W. Lee, Analysis of fracture and deformation modes in teeth subjected to occlusal loading, *Acta Biomater.* 5 (2009) 2213–2221. doi:10.1016/j.actbio.2009.02.001.
- [30] E. Mahoney, A. Holt, M. Swain, N. Kilpatrick, The hardness and modulus of elasticity of primary molar teeth: an ultra-micro-indentation study, *J. Dent.* 28 (2000) 589–594. doi:10.1016/S0300-5712(00)00043-9.
- [31] J. Yan, B. Taskonak, J.J. Mecholsky, Fractography and fracture toughness of human dentin, *J. Mech. Behav. Biomed. Mater.* 2 (2009) 478–484. doi:10.1016/j.jmbbm.2008.12.002.
- [32] M. Lin, F. Xu, T.J. Lu, B.F. Bai, A review of heat transfer in human tooth-Experimental characterization and mathematical modeling, *Dent. Mater.* 26 (2010) 501–513.
doi:10.1016/j.dental.2010.02.009.
- [33] P. Ausiello, S. Rengo, C.L. Davidson, D.C. Watts, Stress distributions in adhesively cemented ceramic and resin-composite class II inlay restorations: A 3D-FEA study, *Dent. Mater.* 20 (2004) 862–872. doi:10.1016/j.dental.2004.05.001.
- [34] L.H. He, M. V. Swain, Nanoindentation derived stress-strain properties of dental materials, *Dent. Mater.* 23 (2007) 814–821. doi:10.1016/j.dental.2006.06.017.
- [35] S. Park, J.B. Quinn, E. Romberg, D. Arola, On the brittleness of enamel and selected dental materials, *Dent. Mater.* 24 (2008) 1477–1485. doi:10.1016/j.dental.2008.03.007.
- [36] D. Bajaj, A. Nazari, N. Eidelman, D.D. Arola, A comparison of fatigue crack growth in human enamel and hydroxyapatite, *Biomaterials.* 29 (2008) 4847–4854.
doi:10.1016/j.biomaterials.2008.08.019.
- [37] F. Toptan, A.C. Alves, B. Henriques, J.C.M. Souza, R. Coelho, F.S. Silva, et al., Influence of the processing route of porcelain/Ti-6Al-4V interfaces on shear bond strength, *J. Mech. Behav. Biomed. Mater.* 20 (2013) 327–337. doi:10.1016/j.jmbbm.2013.02.003.
- [38] B. Henriques, D. Soares, F.S. Silva, Shear bond strength of a hot pressed Au-Pd-Pt alloy-porcelain dental composite, *J. Mech. Behav. Biomed. Mater.* 4 (2011) 1718–1726.
doi:10.1016/j.jmbbm.2011.05.029.

- [39] B. Henriques, M. Sampaio, M. Buciumeanu, J.C.M. Souza, J.R. Gomes, F. Silva, et al., Laser surface structuring of Ti6Al4V substrates for adhesion enhancement in Ti6Al4V-PEEK joints, *Mater. Sci. Eng. C*. 79 (2017) 177–184. doi:10.1016/j.msec.2017.04.157.
- [40] D. Fabris, J.C.M. Souza, F.S. Silva, M. Fredel, J. Mesquita-Guimarães, Y. Zhang, et al., The bending stress distribution in bilayered and graded zirconia-based dental ceramics, *Ceram. Int.* 42 (2016) 11025–11031. doi:10.1016/j.ceramint.2016.03.245.
- [41] J.B. Quinn, G.D. Quinn, J.R. Kelly, S.S. Scherrer, Fractographic analyses of three ceramic whole crown restoration failures, *Dent. Mater.* 21 (2005) 920–929. doi:10.1016/j.dental.2005.01.006.
- [42] L.D. Randolph, W.M. Palin, G. Leloup, J.G. Leprince, Filler characteristics of modern dental resin composites and their influence on physico-mechanical properties, *Dent. Mater.* 32 (2016) 1586–1599. doi:10.1016/j.dental.2016.09.034.
- [43] D.R. Clarke, Interpenetrating Phase Composites, *J. Am. Ceram. Soc.* 75 (1992) 739–758. doi:10.1111/j.1151-2916.1992.tb04138.x.
- [44] J.J. Harris, P.M. Marquis, Comparison of the deformation and failure characteristics of morphologically distinct metal-glass interpenetrating phase composites, *J. Mater. Sci.* 37 (2002) 2801–2810. doi:10.1023/A:1015841721720.
- [45] L.H. He, D. Purton, M. Swain, A novel polymer infiltrated ceramic for dental simulation, *J. Mater. Sci. Mater. Med.* 22 (2011) 1639–1643. doi:10.1007/s10856-011-4350-3.
- [46] B. Kahler, A. Kotousov, M. V. Swain, On the design of dental resin-based composites: A micromechanical approach, *Acta Biomater.* 4 (2008) 165–172. doi:10.1016/j.actbio.2007.06.011.
- [47] C. Chen, F.Z. Trindade, N. De Jager, C.J. Kleverlaan, A.J. Feilzer, The fracture resistance of a CAD/CAM Resin Nano Ceramic (RNC) and a CAD ceramic at different thicknesses, *Dent. Mater.* 30 (2014) 954–962. doi:10.1016/j.dental.2014.05.018.
- [48] V.P. Thompson, D.E. Rekow, Dental ceramics and the Molar Crown Testing Ground, *J Appl Oral Sci.* 12 (2004) 26–36. doi:10.1590/S1678-77572004000500004.
- [49] Y. Wang, N. Katsube, R.R. Seghi, S.I. Rokhlin, Statistical failure analysis of adhesive resin cement bonded dental ceramics, *Eng. Fract. Mech.* 74 (2007) 1838–1856. doi:10.1016/j.engfracmech.2006.11.006.
- [50] J.R. Kelly, Clinically relevant approach to failure testing of all-ceramic restorations., *J. Prosthet.*

- Dent. 81 (1999) 652–661. doi:10.1016/S0022-3913(99)70103-4.
- [51] P. Magne, L.H. Schlichting, H.P. Maia, L.N. Baratieri, In vitro fatigue resistance of CAD/CAM composite resin and ceramic posterior occlusal veneers, *J. Prosthet. Dent.* 104 (2010) 149–157. doi:10.1016/S0022-3913(10)60111-4.
- [52] B.M.A. Al-Makramani, A.A.A. Razak, M.I. Abu-Hassan, Evaluation of load at fracture of procera allceram copings using different luting cements, *J. Prosthodont.* 17 (2008) 120–124. doi:10.1111/j.1532-849X.2007.00270.x.
- [53] C. Kurtoglu, H. Uysal, A. Mamedov, Influence of layer thickness on stress distribution in ceramic-cement-dentin multilayer systems, *Dent. Mater. J.* 27 (2008) 626–632. doi:10.4012/dmj.27.626.
- [54] R.P. Pagniano, R.R. Seghi, S.F. Rosenstiel, R. Wang, N. Katsube, The effect of a layer of resin luting agent on the biaxial flexure strength of two all-ceramic systems, *J. Prosthet. Dent.* 93 (2005) 459–466. doi:10.1016/j.prosdent.2005.02.012.
- [55] M.I. El-Anwar, R. a. Tamam, U.M. Fawzy, S. a. Yousief, The effect of luting cement type and thickness on stress distribution in upper premolar implant restored with metal ceramic crowns, *Tanta Dent. J.* 12 (2015) 48–55. doi:10.1016/j.tdj.2015.01.004.
- [56] R. Wang, N. Katsube, R.R. Seghi, S.I. Rokhlin, Statistical failure analysis of brittle coatings by spherical indentation: Theory and experiment, *J. Mater. Sci.* 41 (2006) 5441–5454. doi:10.1007/s10853-006-0322-2.